Journal of Saudi Chemical Society (2019) **23**, 828–835

King Saud University

Journal of Saudi Chemical Society

www.ksu.edu.sa
www.sciencedirect.com

ORIGINAL ARTICLE

Facile, single-pot preparation of nanoporous SiO_2 particles (carrier) with AgNPs at core and crust for controlled disinfectant release

M. Salman Haider [a,b,c,*], Godlisten Shao [c,g], Ayyaz Ahmad [d], S. Muhammad Imran [c,e], Nadir Abbas [c,f], Ghulam Abbas [b], Manwar Hussain [c], Hee Taik Kim [c]

[a] *Applied Science Research Institute, Korea Advanced Institute of Science and Technology (KAIST), 291 Daehak-ro, Yuseong-gu, Daejeon 34141, Republic of Korea*
[b] *Department of Chemical Engineering, University of Gujrat, HH Campus, 50700 Gujrat, Pakistan*
[c] *Department of Chemical Engineering, Hanyang University, 1271 Sa 3-dong, Sangnok-gu, Ansan-si, Gyeonggi-do 426-791, Republic of Korea*
[d] *Department of Chemical Engineering, Muhammad Nawaz Sharif University of Engineering and Technology, Multan, Pakistan*
[e] *Department of Chemical Engineering, COMSATS University Islamabad, Lahore Campus, Lahore, Pakistan*
[f] *Department of Chemical Engineering, University of Hai'l, Hai'l, Saudi Arabia*
[g] *Department of Chemistry, Mkwawa College, University of Dar es Salaam, P.O. Box 2513 Iringa, Tanzania*

Received 16 October 2018; revised 20 February 2019; accepted 28 February 2019
Available online 11 March 2019

KEYWORDS

SiO_2-AgNPs nanocomposite;
SiO_2-AgNPs @ Core and Crust;
Modified Stöber method;
Silver release;
Antibacterial properties

Abstract This study demonstrates a novel, facile and one-pot approach to synthesize silica nanoparticles with silver at core and crust (SiNP-AgCC). A modified Stöber method was used to make SiNP-AgCC. A significant reduction in the size of SiO_2 nanoparticles was seen, with 2–5 nm AgNPs being uniformly distributed on the surface and 10–20 nm AgNPs in the center. A typical mesoporous SiO_2 particle (SiNP) produced using the Stöber method was transformed to nanoporous SiO_2 by this modified Stöber method. Nanoporous SiO_2 particles with silver in the center are advantageous for slow and consistent Ag^+ release, which was confirmed by Ag^+ ion release test. Antibacterial activities of the samples were tested to evaluate the disinfection performance of the samples on gram-negative bacteria (*Escherichia coli*) using disk diffusion and the LB-agar method. SiNP-AgCC showed prolonged silver release for more than 20 days and improved antibacterial properties even after five days of incubation.
© 2019 King Saud University. Production and hosting by Elsevier B.V. This is an open access article under the CC BY-NC-ND license (http://creativecommons.org/licenses/by-nc-nd/4.0/).

* Corresponding author at: Applied Science Research Institute, Korea Advanced Institute of Science and Technology (KAIST), 291 Daehak-ro, Yuseong-gu, Daejeon 34141, Republic of Korea.
E-mail addresses: salmanhaider@kaist.ac.kr, salman.haider@uog.edu.pk (M.S. Haider).
Peer review under responsibility of King Saud University.

Production and hosting by Elsevier

https://doi.org/10.1016/j.jscs.2019.02.005
1319-6103 © 2019 King Saud University. Production and hosting by Elsevier B.V.
This is an open access article under the CC BY-NC-ND license (http://creativecommons.org/licenses/by-nc-nd/4.0/).

1. Introduction

Silver nanoparticles (AgNPs) have shown effective and wide range antibacterial activity compared to other metal materials [1–5]. Silver and silver-containing materials such as silver nanoparticles (AgNPs) and Ag^+ ions are known to be strong antimicrobial agents. Specifically, Ag^+ ions in aqueous solution have shown pronounced antimicrobial activity, and their antimicrobial mechanism has been studied extensively. Ag^+ ions interact with the proteins on bacterial membranes and can infiltrate bacterial cells, where they interact with DNA and RNA. However, practical applications of AgNPs are often hindered by oxidization of these nanoparticles [6,7], which may cause aggregation and rapid depletion of the source [8–10], ultimately resulting in a loss of antibacterial activity. To solve these problems, inorganic carriers such as zeolite [11], graphene oxide [3], titanium dioxide [12], activated carbon [13] and silica [14] have been investigated as silver-carrying antibacterial agents. Silver can be added to these carriers by electrostatic binding, physical adsorption, or cation exchange. Scheme 1 provides a general schematic diagram for the formation of silica-silver nanoparticles (core and crust).

Silica has attracted great attention as a potential carrier due to its uniform porous structure. SiO_2 nanoparticles have pore diameters ranging from 20 to 100 nm, and have high thermal and chemical stability and large surface area. Silica's porous structure has been investigated widely for controlled drug release in biomedicine [15]. In this study, nanoporous SiO_2 with silver on the surface and in the core was synthesized using the modified Stöber method. The nanoporous structure helps slow the release of Ag^+, increasing the life of this antibacterial material.

2. Materials and methods

2.1. Materials

Ammonium hydroxide NH_4OH (Dae-Jung Chemical and Metal Co. Ltd, Korea, 28.0–30.0%), Tetraethyl orthosilicate (TEOS, Sigma-Aldrich, 98%), 3-(amino propyl) trimethoxysilane (APTMS, Sigma–Aldrich, 97%), formalin (formaldehyde, Sigma–Aldrich, 37% solution in 10–15% methanol), $AgNO_3$ (Sigma–Aldrich, >99.0%), and ethanol (Dae-Jung Chemical, 99.9+%) were purchased and used without further purification.

2.2. Synthesis of SiNP-AgCC

The seeded polymerization method with a sol–gel reaction [3] was used for silica coating of AgNPs, while AgNPs were prepared following previously described methods [3], with appropriate modifications to reduce the particle size. Initially, 1 mL of AgNP stock solution was added to 5 mL of 14.8 M NH_4OH (aq.) solution in ethanol and stirred for 30 min at room temperature. Next, 1 mL TEOS was added to the above solution and stirred for an additional 5 h. Upon completion of the reaction, the solution was diluted with de-ionized water; 0.05 mL of APTMS solution in ethanol and 0.5 mL of 0.004 M $AgNO_3$ were added to the resulting solution, and were stirred for an additional 2 h. Finally, 5 mL of 0.5 M formalin was added to the mixture as the reducing agent. The resulting solution was centrifuged and thoroughly washed with de-ionized water and dried at 60 °C in a vacuum oven for 12 h.

2.3. Characterization

X-ray diffraction (XRD) measurements were performed using a Rigaku rotating anode X-ray diffractometer (D/MAX-2500/PC, Rigaku, Japan) with a scanning speed of 5°/min from 10° to 60° equipped with a Cu-Kα radiation source (λ = 0.15418 nm) at an accelerating voltage of 50 kV and current of 100 mA. The field emission scanning electron microscopy (FE-SEM, Hitachi S-4800 Japan) with an accelerating voltage of 15.0 kV was used to study the morphology of the composite. The FE-SEM was coupled with energy dispersive spectroscopy (EDAX) to assess the purity and elemental composition of the samples that were synthesized in the present study. The sample was sprinkled lightly with a spatula on a carbon tape with an adhesive surface and affixed to an aluminum stub. The sample was then Pt coated by placing the stub into a sputter coater for 10 min to allow a thin layer to form. In addition, Transmission electron microscopy coupled with scanning transmission electron microscopy imaging (STEM) (TEM, Jeol JEM 2100F-Korea) was employed for further study the size and distribution of particles in the samples. To prepare samples for HRTEM imaging, a drop of the solution sample was added to ethanol and sonicated for 30 min before being placed onto a carbon-coated Cu grid (3 nm thick), dried in air and loaded into the electron microscope sample chamber. The Brunauer–Emmett–Teller (BET) surface area and the porosity of the samples were studied by a nitrogen

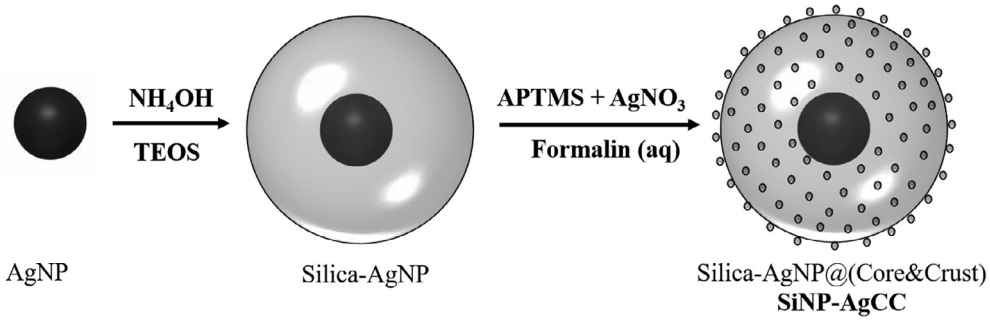

Scheme 1 Schematic illustration of the formation of Silica-AgNPs@ (Core&Crust)/SiNP-AgCC.

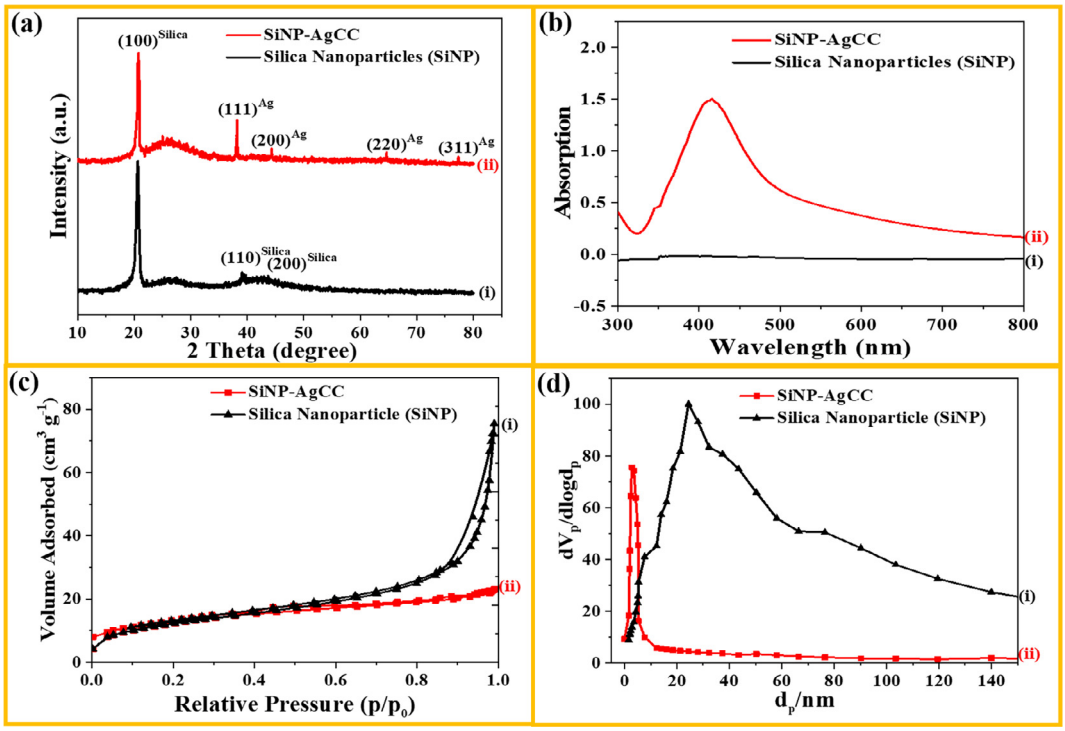

Fig. 1 Comparison between the characteristic properties of SiNP-AgCC and typical Silica nanoparticles (a) XRD (b) UV analysis (c) Pore size distribution of as-synthesized material and (d) Nitrogen adsorption–desorption isotherm.

adsorption instrument (Micrometrics ASAP 2020). All the samples measured were degassed at 200 °C for 2 h prior to actual measurements. Pore size distribution (PSD) and specific desorption pore volumes were obtained using the Barrett–Joyner–Halenda (BJH) method and desorption branches were used to determine the PSD.

2.4. Analytical methods

2.4.1. Ag^+ ion release

The concentration of Ag released from SiO_2-AgNPs was analyzed using dialysis tube method [14,17]. This method of dialysis tubing (Spectra/Por Biotech; cellulose ester; MWCO 14000) was filled with 20 mg of the powdered product dissolved in 10 mL of water, and then immersed in 1000 mL of ultrapure water. Dialysis was carried out under continuous stirring at 37 °C. Periodically, 10 mL of the solution outside the dialysis tubing was removed and the same volume of ultrapure water was added. Silver ion leaching was measured with an inductively coupled plasma optical emission spectrometer (ICP-OES) with axial and radial viewing plasma configuration Model Optima 8000 (Perkin Elmer, USA) operating at a 40 MHz. The nebulization system, with a chemical resistant concentric glass nebulizer coupled to a glass cyclonic spray chamber was utilized. The polychromatic device, with spectral range of 160–900 nm and the system was provided with an S 10 auto sampler (Perkin–Elmer). The operating conditions used are presented in Table S7.

2.4.2. Antibacterial properties (Zone of inhibition Test)

The antibacterial activity of the as-synthesized material was tested against the gram-negative bacterial strain *Escherichia coli* [8]. The gram negative cells were grown in Luria-Bertani medium (Difco™ Laboratories, Detroit, Michigan, USA) acquired from the American type culture collection under the code ATCC 25922, and was maintained at 37 °C with continuous shaking at 180 rpm for 24 h. The antibacterial properties of SiNP-AgCC to constrain the growth of bacteria on the surface of mortar disks were evaluated using zone of inhibition/disk diffusion method (Fig. 5a), using powdered samples (Fig S3), and LB agar plate tests (Fig. 5b), which are the standard microbiological protocols previously used to evaluate antibacterial agents [14]. For the zone of inhibition test, pellets (3 circular pellets 6 mm in diameter) of as-synthesized material were prepared. The sample pellets were dried in a vacuum oven, and 20 µL of the *E. coli* broth culture was spread on the solidified nutrient agar. The sample pellets were placed gently on the agar culture plates and incubated at 37 °C. Simultaneously, powdered SiNP-AgCC were placed gently in a separate agar culture plate to test their efficacy. Finally, a comparative antibacterial test was performed using LB-agar plates. SiO_2 nanoparticles prepared by the typical Stöber method were used as a control. In this test, 10^5 CFU/mL of *E. coli* was incubated with 100 µg of as-synthesized SiNP-AgCC; 50 µg of the complex was spread on the agar plate and bacterial colonies were counted after 24 h.

2.4.3. Concentration-contact testing

To further confirm the enhanced antibacterial properties of as-synthesized material, concentration-contact testing or quantitative suspension test method was also performed [16–18]. In this particular experiment 5 mL of *E. coli* (OD_{600}0.091/mL under the code ATCC 25922) suspended Nutrient broth cultures were made in sterile culture tubes. 1 g of SiNP-AgCC and 1 g of SiO_2 sample were suspended in the bacterial cultures

separately and incubated for 20 min. 100 μL of the culture suspension and four samples were collected at 0th, 5th, 10th and 20th minute of cultivation to investigate the influence of contact time on bacteria. Plating was done with 10^0, 10^2 and 10^4 serial dilutions of the supernatant fractions using nutrient broth. 10 μL of each dilution was plated, in triplicates, on Nutrient agar and incubated at 37 °C for 24 h. Number of colonies formed were counted and converted to CFU/mL. SiO_2 prepared by typical Stöber was used as the control sample tested under the same procedures.

3. Results and discussion

The chemical reduction technique was used for the homogeneous deposition of silver nanoparticles on the surface of silica nanoparticles (SiNP) [3]. This technique is based on the use of a chemical reducing agent (formalin) that allows the reduction of the metal from solution on the surface of the substrate. For this method, the kinetics of electron transfer should be slow enough to avoid the reduction of the metal ions and nucleation in solution (Ag^+ to Ag^0) [17]. The surface (silica nanoparticle) acts then as a scaffold to ensure that reduction only takes place on the surface, so that the metal (Ag^0) remains attached. The XRD patterns of SiNPs prepared by the Stöber method and SiNP-AgCC prepared by the modified Stöber method are shown in Fig. 1a. XRD patterns in Fig. 1a (i) exhibit at least three peaks: (1 0 0), (1 1 0) and (2 1 0). The strong peak at $2\theta = 22°$ indicates the larger pore size of SiO_2 nanoparticles [14–18]. Low intensity peaks at (1 1 0) and (2 0 0) also are distinguishable from the instrumental noise [19]. Prominent peaks corresponding to silver nanoparticles in Fig. 1a (ii) were observed at 38.1°, 44.3°, 64.5° and 77.5°, which can be indexed as (1 1 1), (2 0 0), (2 2 0), and (3 1 1) diffraction peaks of Ag (JCPDS No. 04–0783 "Joint Committee on Powder Diffraction Standards"), respectively [3,20]. Fig. 1a (ii) also exhibits a sharp peak at 220°, indicating SiO_2 nanoparticles. These results confirm the presence of SiO_2 nanoparticles along with AgNPs.

Fig. 1b shows photofluorimetry spectra of SiO_2 nanoparticles and SiNP-AgCC. In Fig. 1b (i), no peak is present in the SiO_2 nanoparticles spectra, indicating the absence of AgNPs, a peak at 405 nm can be observed in the SiNP-AgCC spectra Fig. 1b (ii), indicating the presence of nano-sized silver particles [21].

The mesoporous structure of the SiO_2 nanoparticles prepared by the typical Stöber method and the nanoporous structure of the SiNP-AgCC were confirmed by nitrogen adsorption and desorption isotherms (Fig. 1c). A typical type IV isotherm seen in Fig. 1c (i) confirms the mesoporous structure of silica. In addition, the corresponding pore size distribution curve obtained by the Barrett–Joyner–Halenda (BJH) method using the desorption branch of the isotherm shows a broad peak,

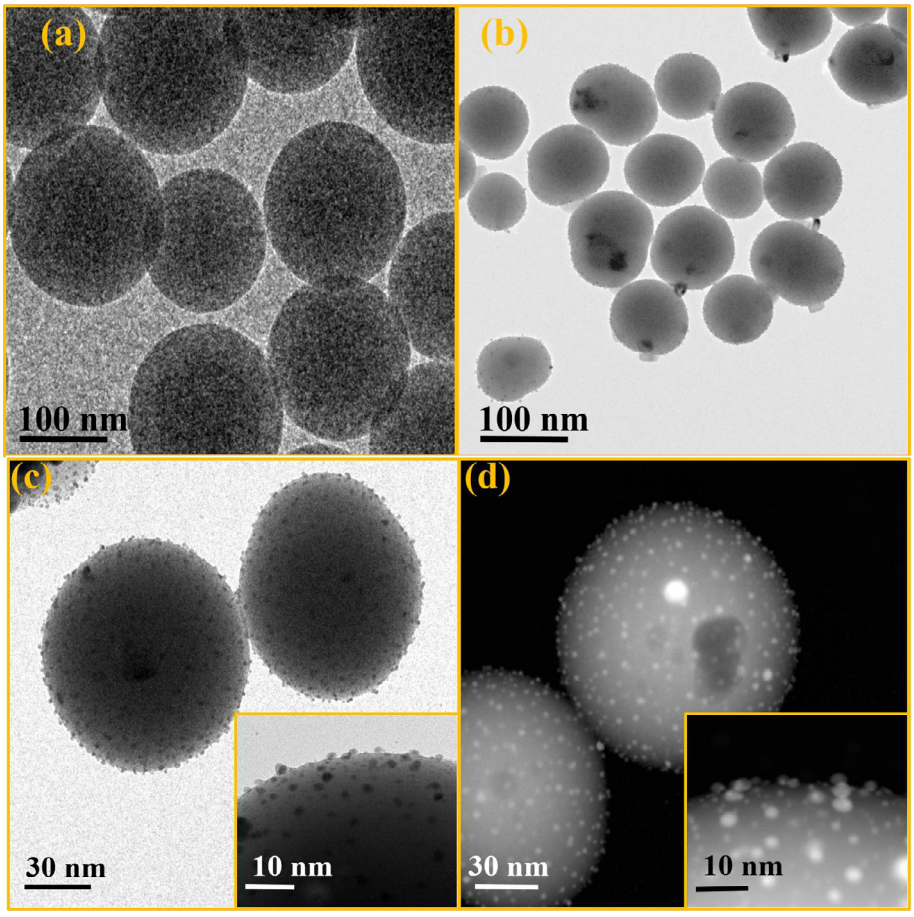

Fig. 2 (a) HRTEM image of SiNP (b) HRTEM image of SiNP-AgCC (c) Magnified HRTEM images of SiNP-AgCC (d) STEM images of SiNP-AgCC.

confirming the average pore diameter greater than 40 nm in Fig. 1d (i). However, in Fig. 1c (ii) the adsorption–desorption curve of SiNP-AgCC possesses a well-defined horizontal plateau at larger relative pressures, with characteristic features of the type I isotherm, indicating a nanoporous structure. Additionally, the pore size distribution curve confirms the presence of nano-sized pores (Fig. 1d (ii)). These results confirm that SiO_2 nanoparticles made by the modified Stöber method are nanoporous silica with AgNPs on the surface and in the core, which is advantageous for slow release of Ag^+ from the particle's core.

HRTEM images of as-synthesized materials are shown in Fig. 2. SiO_2 nanoparticles made using the Stöber method are shown in Fig. 2(a). Based on previous reports [22,23], clear SiO_2 nanoparticles of size 150 nm to 250 nm can be seen. Fig. 2(b) shows an HRTEM image of SiNP-AgCC produced by the modified Stöber method; notably, AgNPs can be seen on the surface and inside the SiO_2 particle. Using this technique, dense particles are formed, which also affects the pore size of SiO_2 particles. Clear differences are apparent in the density of the SiO_2 particles in Fig. 2 (a) and (b); this density change affects the pore size of the SiO_2 particles, resulting in the slow release of Ag^+ ions from the AgNPs at the core of the SiO_2 nanoparticle. Highly magnified HRTEM images are shown in Fig. 2(c). Fig. 2(d) shows STEM images. In both images, uniformly distributed AgNPs 1 nm to 5 nm in diameter can be seen on the surface of the SiO_2 particle, whereas AgNPs 10 nm to 20 nm in diameter can be seen in the center. Fig. S1 shows the particle size distribution of AgNPs in and around SiO_2 particles.

Fig. 3 presents the FESEM results of the as-synthesized SiO_2 nanoparticles and SiNP-AgCC. Fig. 3(a) illustrates a FESEM image of SiO_2 particles prepared by the typical Stöber method, whereas Fig. 3(b) presents a FESEM image of SiNP-AgCC. As can be seen from Fig. 3(a) and (b), there is a clear difference in the size of SiO_2 nanoparticles and SiNP-AgCC. SiO_2 nanoparticles synthesized by the typical Stöber method in this study and in recent previous reports [14,22], were $\geq$200 nm in diameter. Also, based on similar recent reports [14,22], mesoporous SiO_2 nanoparticles (Ag-MSN) synthesized by the Stöber method were $\geq$200 nm in diameter. However, here SiNP-AgCC synthesized by the modified Stöber method was $\leq$100 nm in diameter. This size reduction reduces the pore size of silica, making it nanoporous, and slowing the release of

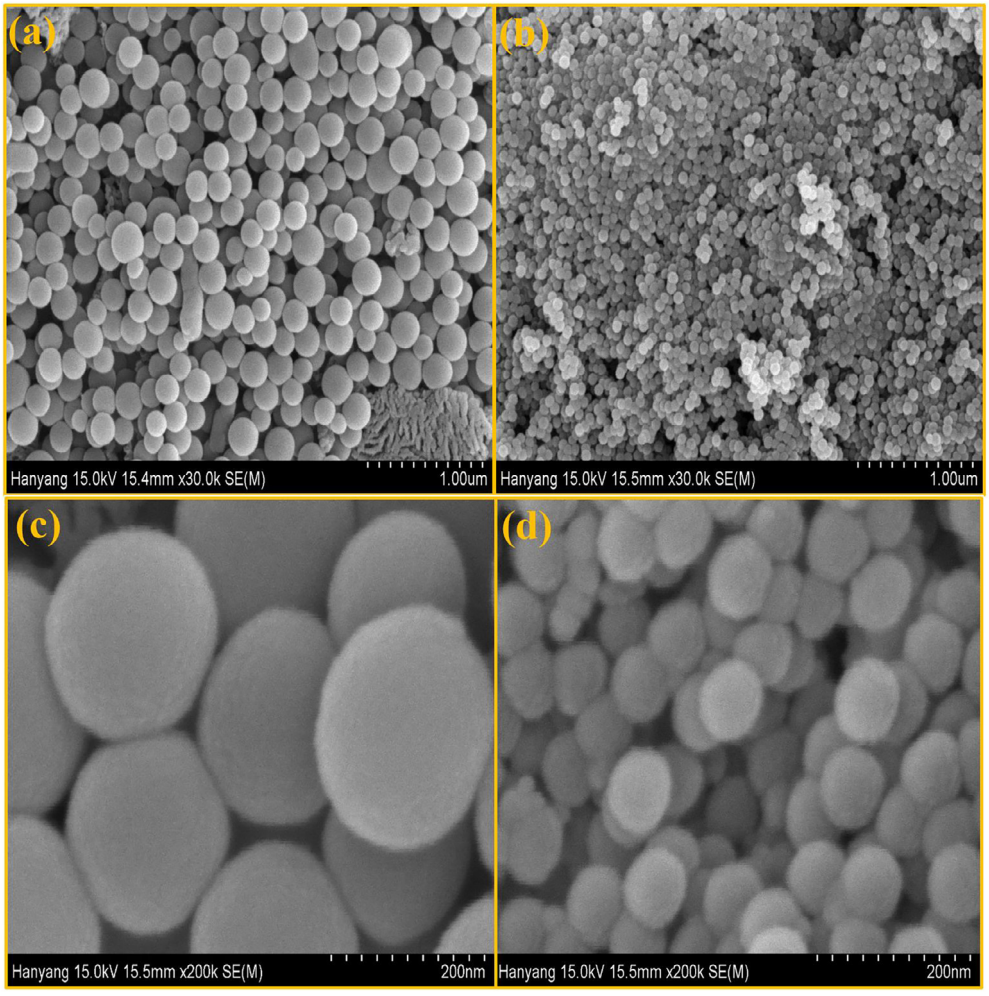

Fig. 3 (a) FESEM images of SiO_2 Nanoparticles and (b) SiNP-AgCC (c) High resolution image of SiO_2 Nanoparticles and (d) High resolution image of SiNP-AgCC.

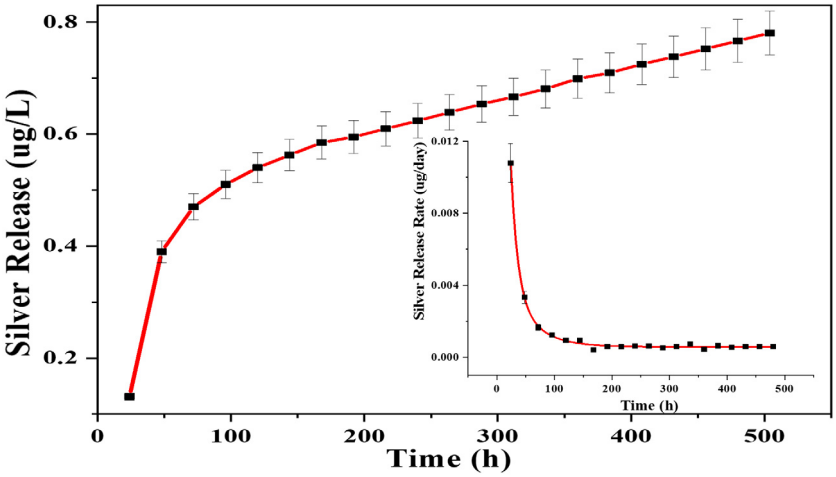

Fig. 4 Silver (Ag+) release and (inset) release rate from SiNP-AgCC at 37 °C during 20 days of continuous dialysis technique.

Ag^+ ions from the AgNPs encapsulated in SiO_2 particles. Fig. 3 (c) and (d) show high magnification images of the same samples, confirming the size reduction achieved using this modified Stöber method. Fig S2 confirms presence of AgNPs in SiO_2 nanoparticles with the EDAX analysis.

3.1. Silver ion (Ag^+) release

The static release of Ag^+ was studied using the immersion technique [8,14] and samples were analyzed by ICP-OES; the results are summarized in Fig. 4. XRD and FESEM results indicated that AgNPs are present in the core and are also well distributed on the surface of the SiO_2 nanoparticles, which act as the carrier, resulting in Ag^+ ion release during dialysis. It can be seen from Fig. 4 that there was a sudden release of silver during the first 48 h; subsequently, silver release was gradual and constant for the next 450 h. The high initial rate in Fig. 4 (inset) is caused by the release of Ag^+ from the AgNPs attached to the surface of the SiO_2 nanoparticles, whereas the gradual rate that followed may have been caused by silver leaching from the core of the SiNP-AgCC. HRTEM images and EDAX graph in Fig. S4(a) evidently shows the presence of silver nanoparticles on surface of SiNP-AgCC nanocomposite before the start of dialysis test. Whereas, in Fig. S4(b) which was analyzed after 15 days of continuous dialysis test the silver nanoparticles on the surface are absent but the presence of silver nanoparticle in the core is confirmed. Fig. S4 and Fig. S5 explains the high Ag^+ ion release during initial 100 h and gradual release after 100 h. The average release rate over the 20-day study period was 0.0015 μg/h, significantly below the WHO standard [24]. BET results confirmed the nanoporous nature of the carrier (silica), adding to the reduced release rate of silver from the core of the SiO_2 nanoparticles.

3.2. Antibacterial properties

Silver is well known for its antibacterial properties [1,3,25,26]. Previous studies have reported that AgNPs ≤20 nm are highly effective disinfectants [27]. The nanocomposite produced in this study was subjected to three types of antibacterial test:

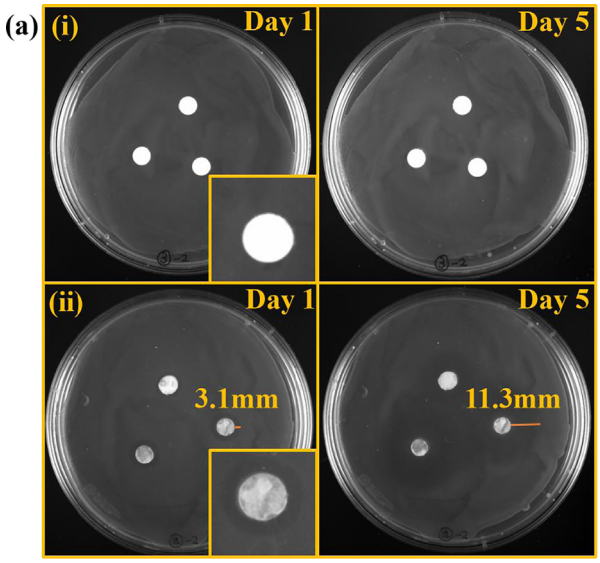

Fig. 5a Zone of inhibition tests of (i) SiO_2 nanoparticles and (ii) SiNP-AgCC using *E. coli* bacteria.

zone of inhibition tests of pellets (Fig. 5a) and powder (Fig. S3), and LB agar plates (Fig. 5b). The presence of the inhibition zone (visible to the unaided eye) is indicative of the antibacterial efficiency of the SiNP-AgCC (Fig. 5a). SiO_2 nanoparticles prepared by the typical Stöber method did not display any antibacterial efficacy, whereas high antibacterial activity was observed in the SiNP-AgCC test. A clear 3.1 mm zone of inhibition was seen after one day, 3.64 times increase (11.3 mm) was observed after five days, confirming the strong bactericidal nature of the as-synthesized material. Fig. S3 also demonstrates that the zone of inhibition can be detected by the unaided eye using powdered samples of SiNP-AgCC. To further show the advantages of this material, we compared the antibacterial properties of SiO_2 nanoparticles, pure AgNPs and as-synthesized SiNP-AgCC using LB agar plate tests (Fig. S6). This also confirmed the superior antibacterial efficacy of the SiNP-AgCC.

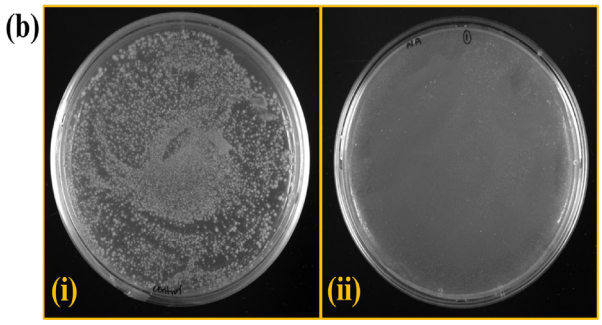

Fig. 5b Bacterial colony growth after 24 h in the presence of as-synthesized material (i) Silica nanoparticles (ii) SiNP-AgCC. In LB-ager inoculated with *E. coli*.

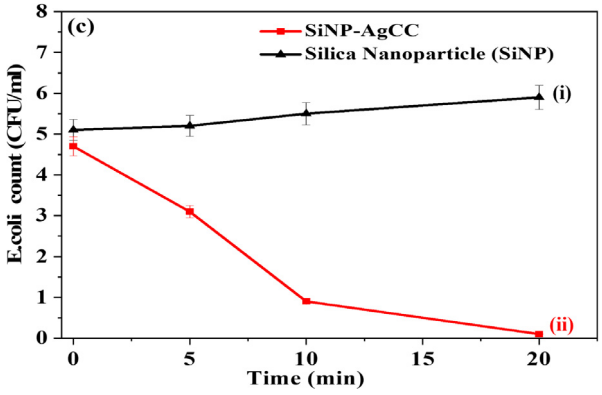

Fig. 5c The concentration/contact test of E. coli colonies on (i) SiNPs and (ii) SiNP-AgCC.

In order to verify the antibacterial properties of material in this particular study; the rate of bacterial inactivation was quantified by concentration/contact testing of *E. coli* colonies and the results are shown in Fig. 5c. The rate of inactivation of *E. coli* was investigated to find out disinfection rate of SiNP-AgCC. In each test, initially 5 mL of *E. coli* bacteria was tested against the samples. SiO_2 showed increase in the count of bacterial colonies which can also be seen in zone of inhibition test, while SiNP-AgCC showed drastic decrease in the count of bacteria. These results are in agreement with the results of zone of inhibition (see Fig. 5a) as anticipated.

4. Conclusions

We describe the synthesis of SiO_2 nanoparticles with AgNPs in the core and uniformly distributed on the surface. The AgNPs on the surface ranged in size from 2 to 5 nm; those at the core ranged from 10 to 20 nm. The nanoporous structure of the carrier (silica) assisted in the slow and controlled released of Ag^+, which continued for more than 20 days under WHO threshold concentrations from Guidelines for Drinking-water Quality. SiNP-AgCC prepared by this method showed strong and persistent antibacterial efficacy, even at very low concentrations. SiNP-AgCC have great potential applications in polymer nanocomposite water treatment membranes [17], as they will not affect the morphology of the membrane; additionally, their biocompatibility makes them appropriate for biomedical use.

Acknowledgement

The authors are thankful to the Korea Institute of Energy Technology Evaluation and Planning (KETEP) from the Ministry of Trade, Industry and Energy of the Republic of Korea through Human Resources Development Program (Grant No. 20124030200130) for supporting this work.

Appendix A. Supplementary data

Supplementary data to this article can be found online at https://doi.org/10.1016/j.jscs.2019.02.005.

References

[1] S. Chernousova, M. Epple, Silver as antibacterial agent: ion, nanoparticle, and metal, Angew. Chem. Int. Edit. 52 (6) (2013) 1636–1653.
[2] M. Rai, A. Yadav, A. Gade, Silver nanoparticles as a new generation of antimicrobials, Biotechnol. Adv. 27 (1) (2009) 76–83.
[3] M.S. Haider, A.C. Badejo, G.N. Shao, S.M. Imran, N. Abbas, Y.G. Chai, M. Hussain, H.T. Kim, Sequential repetitive chemical reduction technique to study size-property relationships of graphene attached Ag nanoparticle, Solid State Sci. 44 (2015) 1–9.
[4] J.A. Lemire, J.J. Harrison, R.J. Turner, Antimicrobial activity of metals: mechanisms, molecular targets and applications, Nat. Rev. Microbiol. 11 (6) (2013) 371–384.
[5] A. Panáček, L. Kvitek, R. Prucek, M. Kolar, R. Vecerova, N. Pizurova, V.K. Sharma, T.j., Nevečná,, R., Zboril,, Silver colloid nanoparticles: synthesis, characterization, and their antibacterial activity, J. Phys. Chem. B. 110 (33) (2006) 16248–16253.
[6] C.-N. Lok, C.-M. Ho, R. Chen, Q.-Y. He, W.-Y. Yu, H. Sun, P. K.-H. Tam, J.-F. Chiu, C.-M. Che, Silver nanoparticles: partial oxidation and antibacterial activities, J. Biol. Inorg. Chem. 12 (4) (2007) 527–534.
[7] D.M. Aruguete, B. Kim, M.F. Hochella, Y. Ma, Y. Cheng, A. Hoegh, J. Liu, A. Pruden, Antimicrobial nanotechnology: its potential for the effective management of microbial drug resistance and implications for research needs in microbial nanotoxicology, Environ. Sci. Process. Impact 15 (1) (2013) 93–102.
[8] M. Zhang, K. Zhang, B. De Gusseme, W. Verstraete, Biogenic silver nanoparticles (bio-Ag 0) decrease biofouling of bio-Ag 0/PES nanocomposite membranes, Water Res. 46 (7) (2012) 2077–2087.
[9] W.-L. Chou, D.-G. Yu, M.-C. Yang, The preparation and characterization of silver-loading cellulose acetate hollow fiber membrane for water treatment, Polym. Adv. Technol. 16 (8) (2005) 600–607.
[10] H. Basri, A.F. Ismail, M. Aziz, K. Nagai, T. Matsuura, M.S. Abdullah, B.C. Ng, Silver-filled polyethersulfone membranes for antibacterial applications — Effect of PVP and TAP addition on silver dispersion, Desalination 261 (3) (2010) 264–271.
[11] K. Kawahara, K. Tsuruda, M. Morishita, M. Uchida, Antibacterial effect of silver-zeolite on oral bacteria under anaerobic conditions, Dent. Mater. 16 (6) (2000) 452–455.
[12] L. Zhang, J.C. Yu, H.Y. Yip, Q. Li, K.W. Kwong, A.-W. Xu, P. K. Wong, Ambient light reduction strategy to synthesize silver nanoparticles and silver-coated TiO2 with enhanced photocatalytic and bactericidal activities, Langmuir 19 (24) (2003) 10372–10380.

[13] S. Zhang, R. Fu, D. Wu, W. Xu, Q. Ye, Z. Chen, Preparation and characterization of antibacterial silver-dispersed activated carbon aerogels, Carbon 42 (15) (2004) 3209–3216.
[14] Y. Tian, J. Qi, W. Zhang, Q. Cai, X. Jiang, Facile, one-pot synthesis, and antibacterial activity of mesoporous silica nanoparticles decorated with well-dispersed silver nanoparticles, ACS Appl. Mater. Interfaces 6 (15) (2014) 12038–12045.
[15] Y. Zhu et al, Stimuli-responsive controlled drug release from a hollow mesoporous silica sphere/polyelectrolyte multilayer core-shell structure, Angew. Chem. 117 (32) (2005) 5213–5217.
[16] T. Koburger et al, Standardized comparison of antiseptic efficacy of triclosan, PVP–iodine, octenidine dihydrochloride, polyhexanide and chlorhexidine digluconate, J. Antimicrob. Chemother 65 (8) (2010) 1712–1719.
[17] M.S. Haider et al, Aminated polyethersulfone-silver nanoparticles (AgNPs-APES) composite membranes with controlled silver ion release for antibacterial and water treatment applications, Mater. Sci. Eng. C Mater. Biol. Appl. 62 (2016) 732–745.
[18] N. Mnasri, C. Charnay, L.-C. de Ménorval, Y. Moussaoui, E. Elaloui, J. Zajac, Micropor. Mesopor. Mat. 196 (2014) 305–313.
[19] C.-M. Yang, C.-Y. Lin, Y. Sakamoto, W.-C. Huang, L.-L. Chang, Chem. Commun. 45 (2008) 5969–5971.
[20] P. Manjari Mishra, S. Kumar Sahoo, G. Kumar Naik, K. Parida, Mater. Lett. 160 (2015) 566–571.
[21] A.Y. Khan, R. Bandyopadhyaya, J. Electroanal. Chem. 727 (2014) 184–190.
[22] Y.-S. Ko, Y.H. Joe, M. Seo, K. Lim, J. Hwang, K. Woo, J. Mater. Chem. B 2 (39) (2014) 6714–6722.
[23] H. Rutledge, B.L. Oliva-Chatelain, S.J. Maguire-Boyle, D.L. Flood, A.R. Barron, Mat. Sci. Semicon. Proc. 17 (2014) 7–12.
[24] WHO, Guidelines, for Drinking-water Quality. World Health Organization 2004 Geneva, Switzerland.
[25] V. Arumugam, M.D. Naresh, R. Sanjeevi, J. Biosciences 19 (3) (1994) 307–313.
[26] M.A. Radzig, V.A. Nadtochenko, O.A. Koksharova, J. Kiwi, V. A. Lipasova, I.A. Khmel, Colloid. Surface B. 102 (2013) 300–306.
[27] J.L. Elechiguerra, J.L. Burt, J.R. Morones, A. Camacho-Bragado, X. Gao, H.H. Lara, M.J. Yacaman, J. Nanobiotechnol. 3 (6) (2005) 1–10.